HOLOGRAM CATR FOR MM- AND SUBMM-WAVELENGTHS: A PROGRESS REPORT

T. Hirvonen, P. Piironen, J. Ala-Laurinaho, A. Lehto, A. V. Räisänen,
Radio Laboratory, Helsinki University of Technology,
P.O.Box 3000, FIN-02015 HUT, Finland
E-mail: thi@radio.hut.fi

Abstract-A development work of a 2.4 m × 2.0 m hologram for testing the 1.1 m offset reflector of Odin satellite at 119 GHz is reported. The design is based on the combination of physical optics (PO) and finite difference time domain (FDTD) method. Feasibility of a submillimeter wave hologram CATR is studied theoretically.

1. Introduction

In a hologram type of compact antenna test range (CATR), the feed horn transmits a spherical wave onto one side of a computer-generated amplitude hologram structure which modulates the field such that a planar wave is emanated on the other side of the structure. The antenna under test (AUT) is illuminated with this plane wave. The extent of the volume enclosing the plane wave is called the quiet-zone. The required field-quality of the quiet-zone is driven by the required measurement accuracy of the AUT. Typical requirements are a peak-to-peak amplitude ripple of less than 1 dB and a peak-to-peak phase ripple of less than 10° in the quiet-zone. The advantage of a hologram is its less stringent surface accuracy requirement than that of a reflector which is the traditional collimating element used in CATRs [1,2]. Figure 1 illustrates a facility layout employing a hologram CATR.

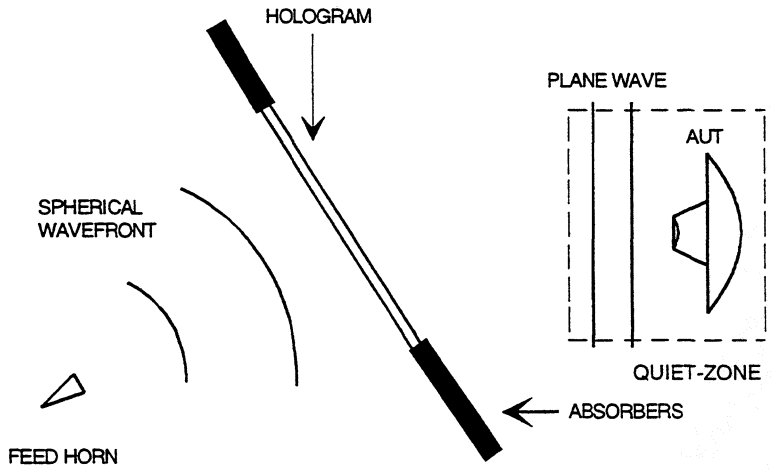

Figure 1. Hologram CATR.

Helsinki University of Technology (HUT) participates in an international, mainly Swedish, Odin satellite project. Odin satellite program is being developed for monitoring aeronomical and astronomical spectral lines. The satellite has a heterodyne receiver at 119 GHz and four heterodyne

receivers at submillimeter wave frequencies between 486 and 580 GHz. The satellite has an offset reflector antenna. The diameter of the main reflector is 1.1 m. The telescope will be tested with a hologram type of a CATR at 119 GHz.

In this paper, the idea of a hologram CATR and the basis of the theoretical analysis are briefly reviewed. The theoretical analysis is based on physical optics (PO) and finite difference time domain (FDTD) method [2,3]. Main emphasis is on the development work of a large 2.4 m × 2.0 m millimeter wave hologram for the Odin telescope tests, and on the current status of the submillimeter wave hologram CATR at HUT.

2. Hologram theory

The binary structure of the amplitude hologram is given (see also [4])

$$T_B(x',y') = \begin{cases} 0, & 0 \le 0.5\left[1+\cos\Psi(x',y')\right] \le b, \\ 1, & b < 0.5\left[1+\cos\Psi(x',y')\right] \le 1, \end{cases} \tag{1}$$

where $b = 1-(1/\pi)\arcsin a(x',y')$. The phase is modulated by the locations of the slots and the amplitude is modulated by the variations of the slot widths. x', y' are the coordinates in the hologram plane, and $0 \le a(x',y') \le 1$ is a real function proportional to the relation between the output and input amplitudes so that the hologram compensates the amplitude variation of the input field and adds an amplitude taper to the amplitude of the output field. The phase term is $\Psi(x',y') = \psi(x',y') + 2\pi\nu x'$, where ν denotes the spatial carrier frequency which separates the diffraction orders produced by the hologram, $\psi(x',y')$ is the normalized phase of the input field in the plane of the hologram. The desired plane wave leaves the hologram at an angle of $\theta = \arcsin(\nu\lambda)$, so that the unwanted diffraction orders do not disturb the quiet-zone of the CATR. The structure of the hologram is derived from the known incident field and the required aperture field, which radiates a plane wave to the quiet-zone. As a result, the hologram consists of narrow curved slots in a conducting plane [2].

The field in the quiet-zone is calculated by using physical optics (PO). The formula for the quiet-zone field is

$$\mathbf{E}(x,y,z) = \int_S E_a(x',y')\frac{1+jkR}{2\pi R^3}e^{-jkR}\left[\mathbf{u}_y(z-z') - \mathbf{u}_z(y-y')\right]dS', \tag{2}$$

where $R = \sqrt{(x-x')^2+(y-y')^2+(z-z')^2}$ is the distance from a point in the aperture to a point in the quiet-zone. In Equation (2), the polarization of the feed antenna is in the $\mathbf{u}_y$-direction. $E_a(x',y')$ is the complex field in the aperture of the hologram. It is calculated with a two-dimensional finite difference time domain (FDTD) analysis. The FDTD prediction is performed across the hologram at a fixed value of y' using the complex field of the feed antenna, in the plane of the hologram, as an excitation. Applying the FDTD analysis incrementally across the entire hologram produces the near-field result which can be integrated (PO) over the hologram surface to

produce the quiet-zone field. Analyzing a single hologram in this way would be prohibitively time consuming taking several months of CPU time on a super computer. However, because the hologram pattern varies slowly with respect to the y'-coordinate, it is sufficient to perform the FDTD analysis at a given $y' = y_n$ and calculate the PO integration over one line in the x-direction, and evaluate the quiet-zone field in the plane at the corresponding $y = y_n$. This analysis was validated by designing, fabricating, and measuring a 55 cm diameter hologram for 119 GHz. The structure of the hologram optimized the quiet-zone field at vertical polarization. Figure 2 shows the theoretical and measured quiet-zone field of the hologram CATR based on the 55 cm diameter hologram. In this case, the optimization was carried out at $y' = 0$ only, and it is more thoroughly reported in [2,3].

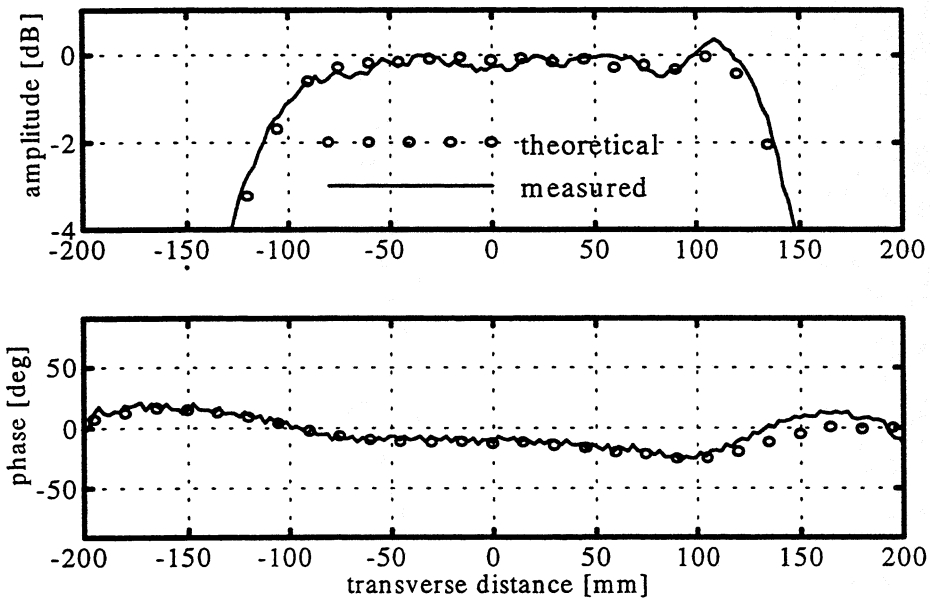

Figure 2. Theoretical and measured quiet-zone field of the 55 cm diameter hologram.

3. Millimeter wave hologram for Odin tests

The purpose of the Odin antenna testing is to verify the radiation pattern of the antenna. In the first phase, during summer of 1997, the radiation pattern of the antenna integrated with the quasioptical feed system will be measured. In the second phase, in the beginning of 1998, the antenna with the quasioptics will be measured after it is mounted on the satellite.

3.1. Hologram design

The size of the facility depends mainly on the required size of the quiet-zone and the way the hologram is illuminated. There is also a slight dependence on the frequency. In this case a 2.4 m × 2.0 m elliptic hologram is designed. The corrugated horn as a feed is placed 6.0 m away from the hologram. The structure of the hologram optimizes the quiet-zone field at vertical polarization 6 m behind the hologram. The plane wave is designed to leave the hologram in an angle of 33.0°. The

thickness of the dielectric film is 75 μm, and the thickness of the copper layer is 35 μm. The relative permittivity of the film is 3.3.

The task of the iterative design procedure is to generate a hologram structure which produces such an aperture field $E_a(x', y')$ which radiates a plane wave to the quiet-zone. The aperture field is calculated with the FDTD analysis after the hologram is generated (Equation (1)). The quiet-zone field is calculated by integrating the aperture field (Equation (2)). Until the quiet-zone field meets the requirements, the hologram needs to be regenerated with changed slot widths and locations in different parts of the hologram. In practice, the problem is to find a proper weighting function $W(x', y')$ for the term $a(x', y') = W(x', y') / \left| E_{\text{feed}}(x', y') \right| \le 1$ which determines the widths of the slots. In the case of the large hologram, the optimization was carried out at $y' = 0$, 250 mm, 500 mm, and 750 mm. The weighting function is as follows

$$W(x', y') = 0.5\cos^{10}\left[\left(\frac{\rho'}{\rho_e'}\right)^6\right]\left[1.7 - 0.9\cos\left(\frac{x'}{1.2}\right)\right] w_1(x') w_2(x'), \tag{3}$$

where

$$\begin{aligned} w_1(x') &= \begin{cases} 0.92 - 0.08\cos[\pi(x'-0.3)/0.5], & -0.2 \le x' \le 0.8, \\ 1.0, & \text{elsewhere}, \end{cases} \\ w_2(x') &= \begin{cases} 1.018 + 0.018\cos[\pi(x'+0.45)/0.3], & -0.75 \le x' \le -0.15, \\ 1.0, & \text{elsewhere}, \end{cases} \end{aligned} \tag{4}$$

and ρ_e' is the radius of the ellipse, and $\rho' = \sqrt{(x'-\xi)^2 + y'^2}$ which means that the hologram is generated asymmetrically in order to have an asymmetric illumination in the x-direction [5]. The phase in the quiet-zone may be tuned by adding an extra phase term to $\Psi(x', y')$ as explained in [2]. In practice, this means that certain parts of the hologram are generated by using a slightly different angle than 33.0° into which the plane wave is launched. In this case

$$\theta = 33.0 \cdot \theta_1(x') \theta_2(x'), \tag{5}$$

where

$$\begin{aligned} \theta_1(x') &= \begin{cases} 1.00004 - 0.00004\cos[\pi(x'+0.25)/0.25], & -0.5 \le x' \le 0.0, \\ 0.99984 - 0.00016\cos[\pi(x'-0.5)/0.3], & 0.2 \le x' \le 0.8, \\ 1.0, & \text{elsewhere}, \end{cases} \\ \theta_2(x') &= \begin{cases} 0.99995 - 0.00005\cos[\pi(x'-0.7)/0.1], & 0.6 \le x' \le 0.8, \\ 1.0, & \text{elsewhere}. \end{cases} \end{aligned} \tag{6}$$

As a result, the hologram consists of 557 curved slots. The widths of the slots are 0.1–1.3 mm. Figure 3 shows the weighting function (Equation (3)) in the x- and y-direction.

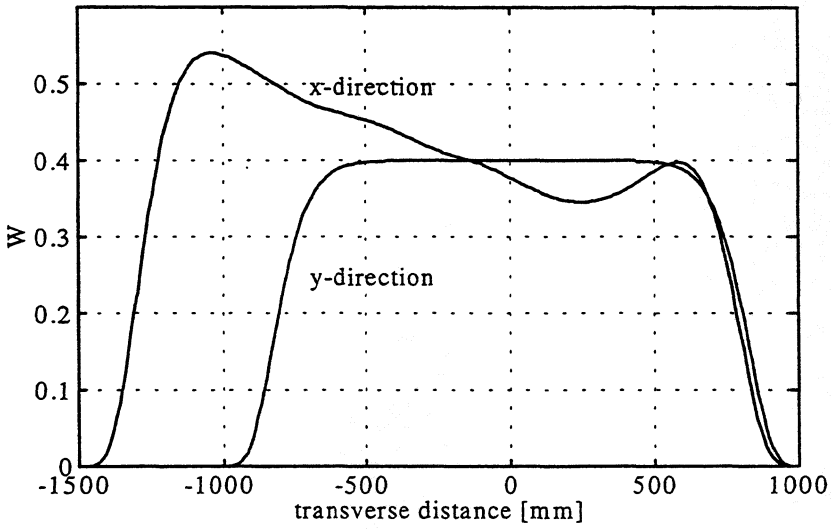

Figure 3. Weighting function in the x- and y-direction.

3.2. Hologram fabrication

The optimized pattern of the hologram is printed on a film with a high-precision plotter. In this case, the resolution is about 760 dots per inch. This film is used as a mask when the pattern is transferred to a copper plated Mylar sheet covered with a photoresist. The fabrication procedure is similar to that used for making printed circuits (silk-screen printing).

The largest size of a high-precision print is 1.2 m × 1.0 m (available in Finland), and 1.0 m wide copper plated Mylar is available. In the pattern transfer and etching procedure, patterns up to about 2.5 m long and over 1 m wide can be fabricated. Furthermore, it is highly desirable to avoid any kind of joints, especially those in the direction of the slots (i.e. vertical), in the center of the hologram. Thus, the hologram is made of three pieces and by using seven masks as shown in Figure 4. The joints of the masks are shown as dashed lines, and the solid lines are the joints between the three pieces. The center part is fabricated by joining three masks together in the pattern transfer process producing a 2.4 m × 1.0 m center part in the etching. The upper and lower parts are fabricated by joining two masks together, respectively. Finally, the three pieces are spliced together by using 50 mm wide and 30 μm thick polyester tape on both sides of the film. The curved lines in Figure 4 illustrate the slots of the hologram.

First version of the 2.4 m × 2.0 m hologram made of three pieces has been fabricated. However, due to unexpected errors in the fabrication, the slots of the hologram are 100–200 μm too narrow producing an erroneous quiet-zone field. Thus, at the moment, only the theoretical quiet-zone field of the large hologram is given, Figure 5. A new, corrected version is under construction.

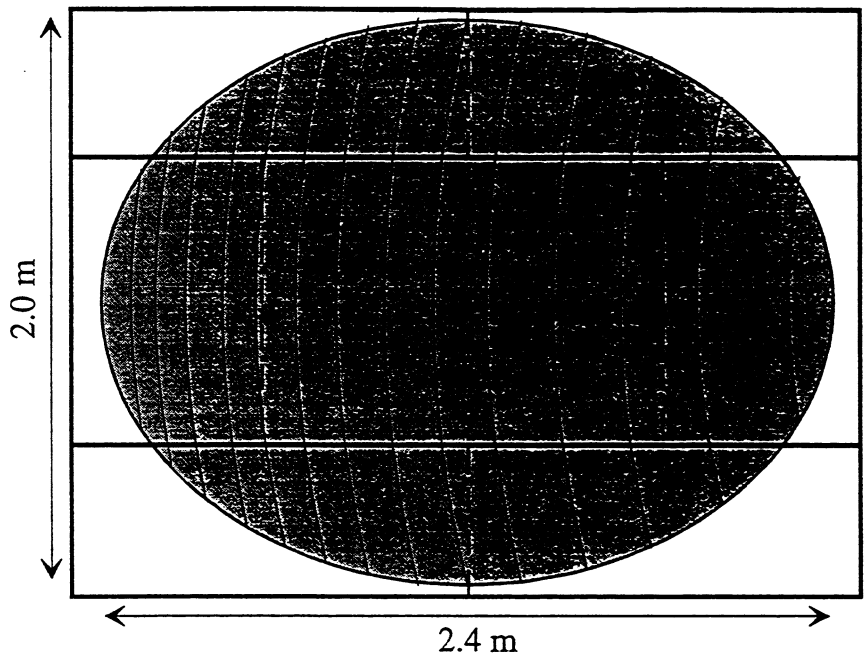

Figure 4. Layout of the hologram fabrication.

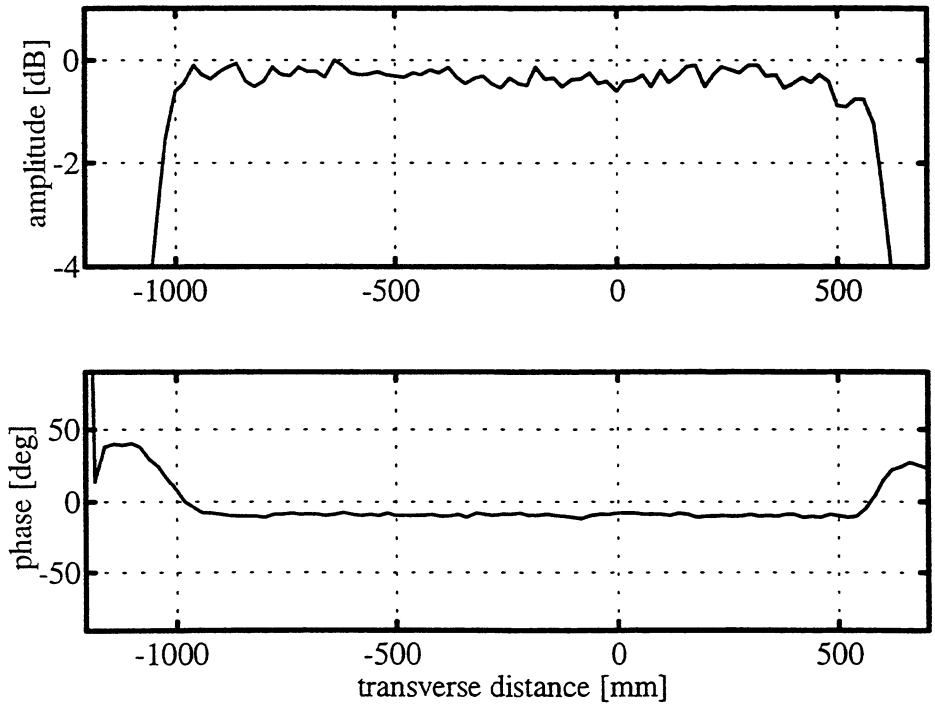

Figure 5. Theoretical quiet-zone field of a CATR employing a 2.4 m × 2.0 m hologram at 119 GHz.

4. Submillimeter wave hologram

The European Space Agency (ESA) is currently examining the use of space-based radiometric instruments to probe the atmosphere in the 200–1000 GHz region. Recently, the Radio Laboratory participated in a study where possible antenna measurement facilities up to 1500 GHz were examined in detail [6]. In this study, the feasibility of a submillimeter wave hologram CATR was theoretically studied by using the combined PO and FDTD method described above. The analyses include the effects of fabrication errors of the hologram pattern and various feed displacements on the quiet-zone field. Also the effect of joints, resulting from the fabrication of the hologram of several pieces, is discussed in [6]. Based on these results, the quality of the attainable quiet-zone at submillimeter wavelengths may be estimated. As an example, part of the results of the performance analysis of a submillimeter wave hologram CATR is given here.

Fabrication errors are due to the inaccuracies of the three main steps in the fabrication procedure: 1) mask (inaccuracy of the printer and the limited size of the graphics file), 2) pattern transfer, and 3) etching. Furthermore, the fabrication errors may be divided into systematic errors and random errors. Due to systematic fabrication errors, all the slots of the hologram are wider or narrower than in an ideal case. Because of the random errors the slots are randomly either wider or narrower than in an ideal case. The order of magnitude of the systematic errors due to each of the three steps of the fabrication procedure may be estimated at 10 μm in the width of the slot. This means that ±30 μm is the worst case, and ±17 μm is the RSS case. The random errors are considered to be due to the limited size of the graphics file or the resolution of the precision printer, and it means that the edges of the curved slots are serrated instead of being smooth. This error is not exactly random but may well be estimated with a normally distributed random error in the widths of the slots. In the case of the millimeter wave hologram [2], this error was measured to be 9 μm. However, a better resolution is achievable.

The effect of these inaccuracies has been estimated at frequencies of 200 and 500 GHz with 20 cm diameter holograms optimized for vertical polarization. In the analysis, the widths of the slots were changed by ±10 μm, ±30 μm , and ±50 μm. The standard deviation in a case of random errors was 5 μm, 10 μm, and 20 μm. The effect of the joints (and gaps) was studied by introducing a 100 μm wide gap in the center of the hologram (at 119 GHz the effects of larger gaps have been studied as well). Figure 6 shows the effect of various fabrication errors on the quiet-zone field compared to the ideal case at 500 GHz. The amplitude curves have been vertically shifted in order to separate them from each other.

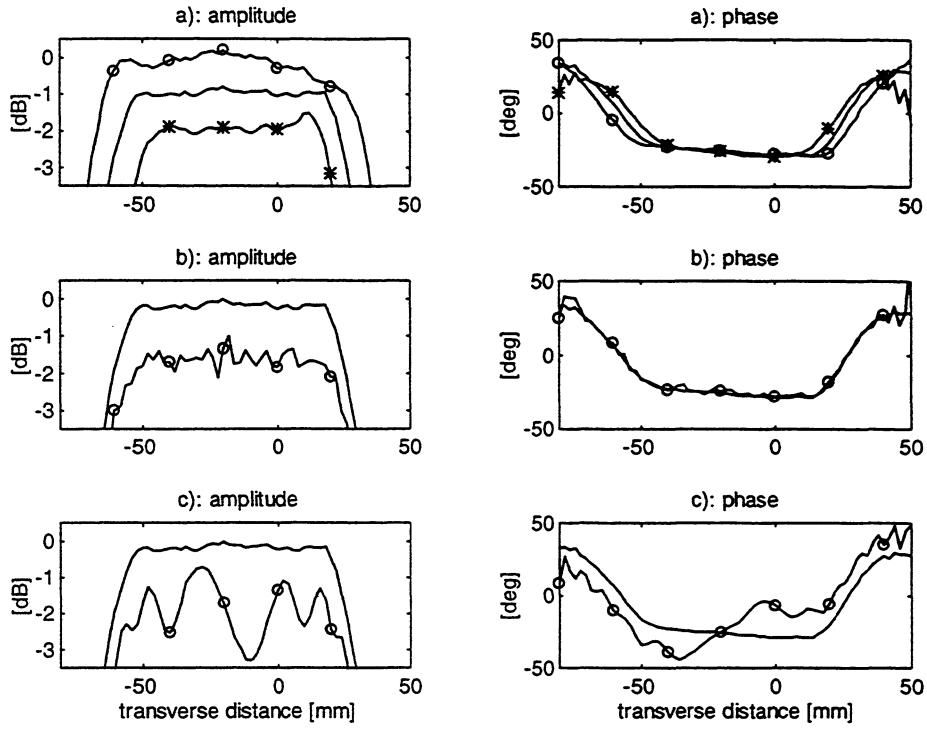

Figure 6. a) Effect of the ± 30 μm systematic fabrication errors: ideal case (-), + 30 μm (o) and – 30 μm (*), b) effect of the random error, σ = 10 μm (o), c) effect of a 100 μm vertical gap in the center of the hologram (o).

The effect of a specific error depends on the frequency, the geometry of the facility (i.e. focal length and diameter of the hologram), and the weighting function. However, these results should give a realistic estimation of the feasibility of a submillimeter wave hologram CATR. Systematic fabrication errors increase slightly the quiet-zone ripple, but the main effect is the change of the size of the quiet-zone. Random errors clearly increase the amplitude and phase ripple in the quiet-zone, and the highest possible resolution of the printer should be utilized. Vertical gaps in the hologram structure have been found to be very undesirable in the development of the 2.4 m × 2.0 m hologram for the Odin tests at 119 GHz. This analysis and those made at 119 GHz confirm that vertical joints should be avoided.

5. Conclusion

A hologram type of compact antenna test range (CATR) utilizes a computer-generated amplitude hologram to form the desired plane wave from the feed horn spherical wave. The analysis method based on physical optics (PO) and finite difference time domain (FDTD) method is validated by comparing the theoretical and experimental results of a CATR employing a 55 cm diameter hologram at 119 GHz. The design, fabrication method, and the theoretical quiet-zone field of a CATR based on a 2.4 m × 2.0 m hologram is presented. Furthermore, feasibility of a submillimeter wave hologram CATR is studied theoretically.

Acknowledgments

The authors are grateful to Mr. Lauri Laakso and Mr. Lorenz Schmuckli for helping in the mechanical aspects related to the testing of the holograms in this work.

6. References

[1] Tuovinen, J., Vasara, A., Räisänen, A.: A new type of compact antenna test range at mm-waves. *Proceedings of the 22nd European Microwave Conference*, Espoo, 1992, pp. 503–508.

[2] Hirvonen, T., Ala-Laurinaho, J., Tuovinen, J., Räisänen, A.: A compact antenna test range based on a hologram. Accepted for publication in *IEEE Transactions on Antennas and Propagation*, 1997.

[3] Ala-Laurinaho, J., Hirvonen, T., Tuovinen, J., Räisänen, A. V.: Numerical modeling of a non-uniform grating with FDTD. Accepted for publication in *Microwave and Optical Technology Letters*, 1997.

[4] Vasara, A., Turunen, J., Friberg, A. T.: Realization of general nondiffracting beams with computer-generated holograms. *Journal of Optical Society of America A,* Vol. 6, 1989, pp. 1748–1754.

[5] Ala-Laurinaho, J., Hirvonen, T., Räisänen, A.: Optimization of a submillimeter wave hologram CATR. To be appeared in *Proceedings of the IEEE AP-S International Symposium*, 1997.

[6] Foster, P. R., Martin, D., Parini, C., Räisänen, A., Ala-Laurinaho, J., Hirvonen, T., Lehto, A., Sehm, T., Tuovinen, J., Jensen, F., Pontoppidan, K.: Mmwave antenna testing techniques–Phase 2. *MAAS Report 304*. ESTEC Contract No 11641/95/NL/PB(SC), 1996.